PAPER

Check for updates

Antifouling activities of pristine and nanocomposite chitosan/TiO₂/Ag films against freshwater algae

Saravanan Natarajan,[a] D. Shanthana Lakshmi,[b] M. Bhuvaneshwari,[a] V. Iswarya,[a] P. Mrudula,[a] N. Chandrasekaran[a] and Amitava Mukherjee [ID] *[a]

Adhesion of microalgae or biofouling on submerged artificial surfaces is a universal problem in freshwater environments. Herein, we developed Ag and TiO₂ nanoparticle (NP)-incorporated nanocomposite and pristine films using chitosan for antifouling applications in freshwater environments. Both TiO₂ and Ag NPs are known for their algaecide activity. Hence, nanocomposite (Ag/TiO₂ and TiO₂/Ag) and pristine (Ag, TiO₂) films containing a range of concentrations of both particles were tested against two freshwater algae, specifically, *Scenedesmus* sp. and *Chlorella* sp. under different photo conditions. The toxicity assays show that *Scenedesmus* sp. is more sensitive to all the films tested than *Chlorella* sp. under both UV-C exposure and dark conditions. The slime formation, biomass (%), LPO, and uptake of the NPs are correlated well with their toxicity data. EPS release is noted to be higher for *Scenedesmus* sp. than *Chlorella* sp. due to the higher toxicity of this algal species. This indicates that the species variation substantially influences the antifouling action of both the pristine and nanocomposite films.

1. Introduction

Biofouling is the formation of an interface between man-made surfaces and fouling organisms such as barnacles, bacteria, macro and micro algae[1] in both marine and freshwater environments.[2] The use of biocidal metal-based antifouling paints in aquatic environments, such as those containing tributyltin and triphenyltin,[3] has been banned for naval application since 2003.[4,5] A cost-effective and simple solution for fouling with minimal toxicity is still an unfulfilled goal despite significant research efforts.

Polymeric antifouling coatings are advanced materials with easy application.[6,7] There are three major reasons for the use of antifouling coating polymers: controlling fouling organism growth, minimizing the adhesion of foulants and preventing biofouling organisms attaching to surfaces.[8,9] Chitosan is reported to exhibit excellent antimicrobial properties[10] due to its cationic nature, charged groups in its polymer backbone and ionic interactions with algal cell wall. The deacetylation of chitin enhances the antibacterial and algaecidal activity of metal oxide nanoparticles thus making nanocomposites effective antimicrobial materials.[11–13] Ren *et al.* (2014) reported the fouling-resistant behaviour of AgNP–PDA-modified surfaces against two typical fouling organisms: the marine microalga

Dunaliella tertiolecta and a freshwater green algal community. They observed that the inhibitory effect of Ag NPs against the adhesion of microalgae was above 85% in both seawater and freshwater environments.[4]

Metal oxide nanoparticle-based coatings play a vital role in the non-toxic control technologies for aquatic organisms.[1] Photocatalytic TiO₂ NPs are one of the most promising antimicrobial agents.[14] TiO₂ nanoparticles generate electron–hole pairs when exposed to UV light, which produce free radicals *via* photo-generated holes and electrons on TiO₂ surfaces. Ag NPs containing biocides and water repellents have excellent algaecide activity, which depends on the Ag concentration or other chemical combinations.[15] Modified TiO₂ catalysts limit the electron–hole recombination and enhance photocatalytic ability with the help of nanoparticles such as Sn, Au, Ag, and Pt.[16] Dineshram *et al.* (2009) considered the application of ultraviolet (UV) radiation as one of the promising methods for the control of biofouling. Employing UV-C radiation is quite advantageous as it is less harmful compared to biocides and requires no physical contact with the targeting surface, thereby reducing abrasion.[1]

In this present study, the antifouling activity of chitosan/TiO₂/Ag composite films against freshwater algal isolates, *Chlorella* sp. and *Scenedesmus* sp., under UV-C and dark conditions is investigated. The possible mechanism of antialgal action is studied *via* the ROS and LPO release by algal cells upon exposure to pristine and nanocomposite films (TiO₂, Ag, TiO₂/Ag and Ag/TiO₂). The EPS formation on the nanocomposite film and the adhesion of algal biomass are quantified. Additionally, the dissolution of Ag NPs and uptake of Ag and Ti NPs into the

[a]Centre for Nanobiotechnology, VIT University, Vellore-632 014, India. E-mail: amit.mookerjea@gmail.com; amitav@vit.ac.in; Fax: +91 416 2243092; Tel: +91 416 2202620

[b]Reverse Osmosis Membrane Division, CSIR-Central Salt and Marine Chemicals Research Institute (CSIR-CSMCRI), Council of Scientific and Industrial Research (CSIR), G. B. Marg, Bhavnagar-364 002, Gujarat, India

cells are quantified. FT-IR and XRD analysis are used to study the characteristics of the nanocomposite films before and after interaction with freshwater algal isolates.

2. Materials and methods

2.1 Chemicals

BG-11 medium, toluidine blue, trichloroacetic acid, and tetraboric acid were procured from Hi-media Laboratories Pvt. Ltd. (Mumbai, India). TiO_2 NPs, Ag NPs, phenol sulphuric acid and chitosan were purchased from Sigma-Aldrich.

2.2 Preparation of nanocomposite and pristine films

Nanocomposite Ag/TiO_2 films and pristine TiO_2 and Ag films (composition details presented in Table 1) were prepared according to our previous report but with varying quantities of both Ag and TiO_2 particles in the present study.[24] In detail, a 3 wt% chitosan solution was prepared by dissolving chitosan in acetic acid. A high-speed ultrasonic probe sonicator (Oscar ultrasonic cleaner, Microclean-109) was used to disperse the nanoparticles (TiO_2 and Ag) for 20 min to obtain a homogenous solution. Different concentrations of Ag and TiO_2 nanoparticle colloidal solutions were mixed with chitosan solution. The solution (chitosan with nanoparticles) was then poured into a clean glass Petri plate and dried at 40 °C in a hot air oven for 24 h. After drying, the chitosan nanoparticle film was peeled off from the plate and stored in a desiccator for further use.

2.3 Toxicity assessment

The freshwater microalgae *Chlorella* sp. and *Scenedesmus* sp. were employed as test strains for the assessment of algaecide effect. The algal cells were grown in a BG-11 medium in a day/night cycle of 12 h/12 h at 20 °C with light illumination of 3000 lux using white fluorescent lights (TL-D Super 80 Linear fluorescent tube, Philips, India).[17–19] At the exponential stage of growth, the *Chlorella* sp. and *Scenedesmus* sp. cells were harvested by centrifugation at 7000 rpm for 10 min, and the obtained pellet was washed thoroughly in sterile BG-11 medium. 10 mL of 0.1 OD algal cells interacted with 1 cm^2 × 1 cm^2

pristine and nanocomposite films for 72 h under UV-C light (intensity of 0.44 mW cm^{-2}, wavelength < 280 nm, TUV 15W/G15 T8, Philips, India)[17] and in dark (covered with an opaque sheet) conditions. The different concentrations of pristine and nanocomposite films are specified in Table 1. After an interaction period of 72 h, the interacted cells were counted on a hemocytometer under an optical microscope (Zeiss Axiostar Microscope, USA). In the treated cells, the percentage reduction in cell viability was calculated with respect to control cells (devoid of any NPs), and the blank film containing only chitosan was used as the positive control.

2.4 Uptake/internalisation of TiO_2 and Ag into *Chlorella* sp. and *Scenedesmus* sp.

The algal cells interacted with pristine and nanocomposite films were centrifuged at 7000 rpm for 10 min and the pellet obtained was used to evaluate the intracellular metal content.[20] The algal samples were acid digested using concentrated HNO_3, and the internalised Ag and TiO_2 were quantified using the graphite furnace method (Analyst 400, PerkinElmer) at a wavelength of 334.94 and 325 nm for TiO_2 and Ag, respectively.

2.5 Lipid peroxidation assay

Lipid peroxidation (LPO) was determined in both freshwater algae after 72 h interaction with the pristine and nanocomposite films under dark and UV-C conditions.[21] In brief, the interacted algal cells were harvested by centrifugation at 10 000g for 10 min, and the resulting pellet was treated with 0.25% (w/v) TBA in 10% (w/v) TCA. After heating at 95 °C for 30 min, the mixture was cooled and centrifuged. The absorbance at 532 nm was recorded using a UV-vis spectrophotometer and any unspecific turbidity measured at 600 nm was subtracted from the absorbance.

2.6 Exo-polymeric substance (EPS)

EPS formation in the algal cells treated with the pristine and nanocomposite films was studied according to Dalai *et al.* (2013). The treated and untreated algal cells were centrifuged at 10 000g for 10 min and pre-chilled ethanol added and then the cells were left at 4 °C overnight to precipitate the EPS. The precipitation and washing were done twice. EPS quantification was done using the phenol–sulphuric acid method.[22]

2.7 Mass assessment

Each of the pristine and nanocomposite films was weighed before and after interaction with the algal cells to ascertain changes in their weight%. The interacted films were rinsed with Milli-Q water and allowed to dry until their weight remained constant. The biomass of algal cells and weight of slime formed (exopolysaccharides) on chitosan (blank), pristine, and nanocomposite film were calculated as mean mass values.[23]

2.8 Slime test

Slime (glycocalyx) formation on the pristine and nanocomposite films was assessed through a series of fixation and staining

Table 1 The compositions and concentrations of the chitosan nanocomposite and pristine films

Film	Ag concentration (wt%)	TiO_2 concentration (wt%)
Chitosan blank	—	—
Composite A	0.5	0.1
Composite B	0.5	0.5
Composite C	0.5	0.75
Pristine D	—	0.1
Pristine E	—	0.5
Pristine F	—	0.75
Composite G	0.1	0.5
Composite H	0.75	0.5
Pristine I	0.1	—
Pristine J	0.5	—
Pristine K	0.75	—

steps. The algal cell-interacted pristine and nanocomposite films containing surface-attached glycocalyx were washed with 1 mL of deionized water before staining. The pristine and nanocomposite films containing slime were initially reacted with Carnoy's solution in a 6 : 3 : 1 ratio of absolute ethanol, chloroform, and glacial acetic acid for 30 min. After the interaction, the Carnoy's solution was removed and the produced slime present on the polymer film was stained using 0.1% of toluidine blue for 1 h. The films were rinsed with Milli-Q water to remove excess stain, and 0.2 M of NaOH was then added and heated at 85 °C for 1 h. The obtained solution was allowed to cool to room temperature and its absorbance was measured at 590 nm using a UV-vis spectrophotometer.[23]

2.9 Chitosan nanocomposite films characterization

2.9.1 Functional group changes analysed by FTIR. Fourier transform infrared spectroscopy was used to analyse the changes in functional groups before and after the interaction[24] in their native form. The spectra were recorded in the range of 4000–600 cm^{-1} (Fourier transform infrared spectrometer, Shimadzu, Japan).

2.9.2 X-ray diffraction (XRD). The diffraction patterns of the TiO$_2$/Ag NP-incorporated nanocomposite and pristine films were assessed using XRD (PAN analytical Xpert Pro MRD diffractometer, Amsterdam, Netherlands), equipped with Cu radiation at a wavelength of 0.15406 nm. The pristine and nanocomposite films after the interaction period of 72 h were scanned over the 2θ range of 10–50° at a scanning rate of 0.5° min^{-1} at room temperature.

2.10 Dissolution of Ag$^+$ from nanocomposite film

Atomic absorption spectroscopy was used to quantify the Ag ions released from the TiO$_2$/Ag nanocomposite and pristine Ag films.[17] The nanocomposite film with the size of 1 cm^2 × 1 cm^2 was cut and immersed in 10 mL of BG-11 media under abiotic conditions for 72 h. After the interaction period, the suspensions containing the released Ag$^+$ ions were centrifuged at 12 000 rpm for 20 min. The centrifuged supernatant was filtered through a 0.1 μm filter, followed by a 3 kDa filter and the released Ag ions present only in the filtered content was used for further quantification of Ag$^+$ using AAS.

2.11 Statistical analysis

All the assessed values are mentioned as mean ± SE. The data were analysed using two-way ANOVA to determine the significance of the various exposure conditions and the different titanium and silver nanoparticles concentrated film toxicities. Statistical significance was accepted at a level of $P < 0.05$.

3. Results

3.1 Antialgal activity

Toxicity due to the nanocomposite and pristine films (Ag/TiO$_2$, TiO$_2$/Ag, Ti, and Ag) was evaluated under dark and UV-C conditions on the freshwater algal test organisms *Chlorella* sp. and *Scenedesmus* sp. (Fig. 1).

On *Chlorella* sp., the toxicity of the nanocomposite films Ag/Ti (A, B and C) was found to be 20.95 ± 0.95%, 35.24 ± 4.47% and 35.76 ± 8.07% and 52.2 ± 5.04%, 56.09 ± 4.62% and 61.29 ± 8.35% under dark and UV-C conditions, respectively. For the nanocomposite films of Ti/Ag (H and G), toxicity was found to be 31.05 ± 1.82% and 26.77 ± 0.621% and 50.26 ± 5.61% and 45.69 ± 2.83% under dark and UV-C conditions, respectively. For the pristine Ti (D, E and F) films toxicity was noted to be 17.19 ± 3.35%, 30.71 ± 7.63% and 33.1 ± 3.87% and 22.89 ± 5.04%, 47.32 ± 2.67% and 51.47 ± 1.47% under dark and UV-C conditions, respectively. The toxic effect of the pristine AgNP (I, J and K) films was found to be 6.68 ± 9.75%, 13.95 ± 9.33% and 21.21 ± 3.4% (dark) and 29.56 ± 2.78%, 35.76 ± 5.4% and 42.85 ± 7.14% (UV-C), respectively.

The film toxicity on *Scenedesmus* sp. under dark and UV-C conditions with respect to the control was measured. For the Ag/Ti (A, B and C) films, their toxicity under dark conditions was found to be 49.94 ± 3.39%, 60.17 ± 0.17% and 65.25 ± 0.25% and UV-C was 72.43 ± 10.89%, 71.89 ± 7.27% and 85.78 ± 0.36%, respectively. The Ti/Ag (H and G) nanocomposite toxicity under UV-C conditions was observed to be 73.38 ± 0.46% and 73.65 ± 1.34% and dark conditions was 60.14 ± 1.52% and 50.89 ± 2.55%, respectively. In the case of the pristine Ti films (D, E and F), their toxicity evaluated under UV-C irradiation was 78.09 ± 7.32%, 86.10 ± 7.64% and 90.99 ± 4.83% and in the dark was 50.05 ± 3.39%, 69.48 ± 0.51% and 72.09 ± 3.76%, respectively. The pristine Ag (I, J and K) film toxicity was observed to be 53.39 ± 0.05%, 61.86 ± 0.2% and 72.81 ± 3.85% in the dark and 67.90 ± 7.48%, 73.87 ± 3.04% and 77.22 ± 4.31% under UV-C, respectively.

Both the nanocomposite and pristine films (Ag/TiO$_2$, TiO$_2$/Ag, Ti, and Ag) showed significantly higher toxicity to *Scenedesmus* sp. than to *Chlorella* sp. under both UV-C and dark conditions at all exposure concentrations ($P < 0.001$). A concentration-dependent increase in the loss of cell viability for *Chlorella* sp. was observed upon exposure to the pristine TiO$_2$ films under UV-C exposure ($P > 0.05$), whereas an insignificant difference was observed under dark conditions ($P > 0.05$). In contrast, the pristine Ag films did not show any significant difference between exposure concentrations under both UV-C and dark conditions on *Chlorella* sp. ($P > 0.05$). The exposure of *Scenedesmus* sp. to the pristine Ag and TiO$_2$ films did not result in any concentration-dependent increase in toxicity under both UV-C and dark conditions ($P > 0.05$).

As the concentration of TiO$_2$ NPs increased (Ag NPs constant), the loss of cell viability for *Chlorella* sp. and *Scenedesmus* sp. also increased significantly ($P < 0.001$) under both UV-C and dark conditions with exposure to the nanocomposite Ag/TiO$_2$ films (A, B and C). Similarly, as the concentration of Ag NPs increased (TiO$_2$ NPs constant), the nanocomposite TiO$_2$/Ag films (H and G) also showed an increase in toxicity under both UV-C and dark conditions ($P > 0.05$). However, there was no significant difference between the nanocomposite films of Ag/TiO$_2$ (A, B, and C) and TiO$_2$/Ag (G, H) under both UV-C and dark conditions ($P > 0.05$).
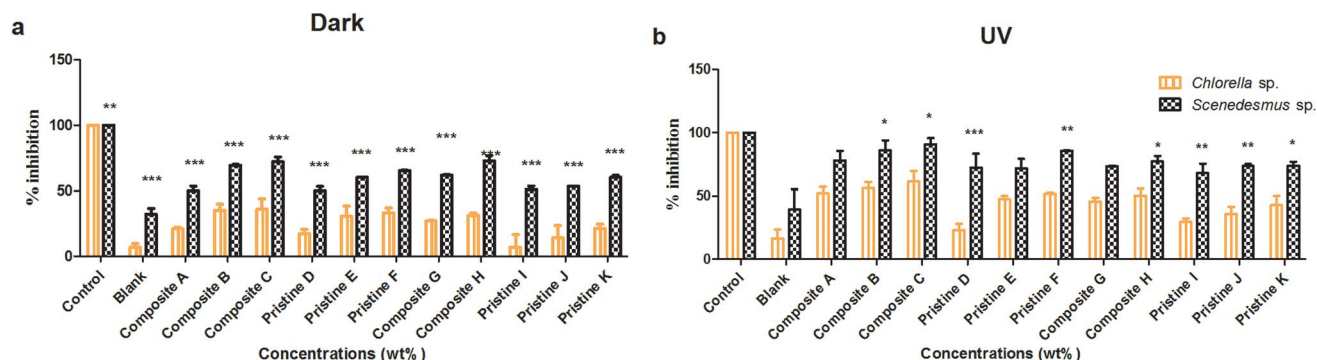
Fig. 1 Cell viability assessment showing the concentration-dependent increase in toxicity under UV-C and dark conditions. The data are presented as mean ± SE, $n = 3$. Asterisks denote statistical significance ($P < 0.001$).

3.2 Antifouling activity

3.2.1 Slime formation.
The slime test (adhesion of microalgae on the surface of the films) for the nanocomposite and pristine films was conducted under dark and UV-C conditions for *Chlorella* sp. and *Scenedesmus* sp. (Fig. 2). The slime activity of the nanocomposite Ag/TiO$_2$ (A and C) films on *Chlorella* sp. was measured to be 0.274 ± 0.007 and 0.232 ± 0.003 AU and 0.233 ± 0.007 and 0.194 ± 0.001 AU under dark and UV-C conditions, respectively. The nanocomposite TiO$_2$/Ag films (H and G) showed slime activity of about 0.276 ± 0.007 and 0.295 ± 0.002 AU and 0.253 ± 0.003 and 0.289 ± 0.005 AU under dark and UV-C conditions, respectively. The adhesion of the pristine TiO$_2$ films (D and F) was observed to be 0.205 ± 0.004 and 0.253 ± 0.003 AU under UV-C and 0.228 ± 0.002 and 0.278 ± 0.008 AU in the dark, respectively. In case of the pristine Ag films (K and I), the slime formation was found to be 0.284 ± 0.006 and 0.311 ± 0.007 AU and 0.275 ± 0.002 and 0.309 ± 0.002 AU under dark and UV-C conditions, respectively.

For *Scenedesmus* sp., the pristine TiO$_2$ films (F and D) showed slime activity of about 0.136 ± 0.002 and 0.167 ± 0.003 AU and 0.123 ± 0.002 and 0.145 ± 0.003 AU under dark and UV-C conditions, respectively. The pristine Ag films (K and I) showed slime formation of about 0.157 ± 0.004 and 0.183 ± 0.002 AU and 0.156 ± 0.004 and 0.144 ± 0.002 AU under dark and UV-C conditions, respectively. The nanocomposite Ag/TiO$_2$ films (C and A) showed slime activity of about 0.103 ± 0.002 and 0.139 ± 0.002 AU and 0.122 ± 0.002 and 0.153 ± 0.003 AU under UV-C and dark conditions, respectively. The nanocomposite TiO$_2$/Ag (H and G) films showed slime activity of about 0.153 ± 0.003 and 0.122 ± 0.001 AU and 0.150 ± 0.006 and 0.178 ± 0.003 AU under dark and UV-C conditions, respectively.

The nanocomposite and pristine films (Ag/TiO$_2$, TiO$_2$/Ag, TiO$_2$, and Ag) significantly showed less slime production on *Scenedesmus* sp. compared to *Chlorella* sp. under both UV-C and dark conditions at all exposure concentrations ($P < 0.001$). There was no significant difference in slime production by *Chlorella* sp. between the UV-C and dark conditions ($P > 0.05$), except for the nanocomposite Ag/TiO$_2$ (A, B and C) films ($P < 0.001$). Similarly, there was no significant difference in slime production by *Scenedesmus* sp. between the UV-C and dark conditions ($P > 0.05$), except for the nanocomposite Ag/TiO$_2$, TiO$_2$/Ag and pristine TiO$_2$ (B, C, D, F and G) films ($P < 0.001$). The dark conditions showed higher slime formation compared to that under UV-C exposure. A concentration-dependent decrease in slime production by *Scenedesmus* sp. was observed upon exposure to the pristine TiO$_2$ films under UV-C and dark conditions ($P < 0.001$).

As the concentration of the TiO$_2$ NPs increased (Ag NPs constant), a decrease in slime formation was noted in the case of both *Scenedesmus* sp. and *Chlorella* sp. ($P < 0.001$) under UV-C
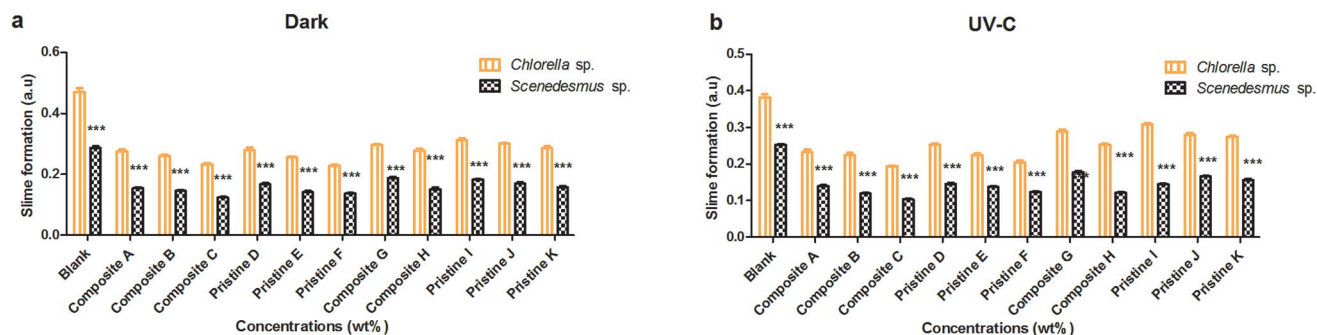

Fig. 2 The level of slime formation on the nanocomposite and pristine films upon interaction with *Chlorella* and *Scenedesmus* sp. under (a) dark and (b) UV-C conditions. The data are presented as mean ± SE, $n = 3$. Asterisks represent the level of significance ($P < 0.01$) between *Chlorella* and *Scenedesmus* sp.

and dark conditions for the nanocomposite Ag/TiO$_2$ films (A, B and C). Similarly, as the concentration of Ag NPs increased (keeping the concentration of the TiO$_2$ NPs constant), the TiO$_2$/Ag films (G and H) showed a decrease in slime formation under both UV-C and dark conditions ($P < 0.001$). There was a significant difference between the treatments with the nanocomposite films of Ag/TiO$_2$ (A, B and C) and TiO$_2$/Ag (G and H) under both UV-C and dark conditions ($P < 0.001$); whereas, film G showed an insignificant ($P > 0.05$) difference in comparison with the nanocomposite films A and B in the dark for *Chlorella* sp. For *Scenedesmus* sp., the nanocomposite C film showed an insignificant ($P > 0.05$) difference with respect to the film A under dark conditions and film B under both conditions.

3.2.2 Mass assessment. Mass assessment of the composite and pristine films that interacted with *Chlorella* sp. and *Scenedesmus* sp. under dark and UV-C conditions was conducted (Fig. 3). The *Chlorella* sp. interacted nanocomposite Ag/TiO$_2$ (C and A) films showed a mass of about 0.745 ± 0.0025 and 1.420 ± 0.001 mg and 1.380 ± 0 and 0.43 ± 0.001 mg under dark and UV-C conditions, respectively. The mass of the nanocomposite TiO$_2$/Ag films (G and H) was measured to be 0.595 ± 0.003 and 0.980 ± 0 mg and 0.43 ± 0.001 and 0.295 ± 0 mg under dark and UV-C conditions, respectively. The pristine Ag films (K and I) showed mass values of about 0.090 ± 0 and 0.685 ± 0 mg and 0.355 ± 0 and 1.110 ± 0 mg under UV-C and dark conditions, respectively. The mass of the pristine TiO$_2$ films (F and D) was observed to be 0.540 ± 0 and 0.585 ± 0 mg and 0.490 ± 0 and 0.685 ± 0 mg under dark and UV-C conditions, respectively.

Mass assessment of the nanocomposite and pristine films with *Scenedesmus* sp. was also performed under dark and UV-C conditions. The mass of the pristine TiO$_2$ films (F and D) was measured to be 0.020 ± 0 and 0.110 ± 0 mg and 0.135 ± 0 and 0.525 ± 0 mg under UV-C and dark conditions, respectively. The pristine Ag films (K and I) showed the mass of about 0.125 ± 0 and 0.335 ± 0 mg and 0.105 ± 0 and 0.250 ± 0 under dark and UV-C conditions, respectively. The mass of the nanocomposite Ag/TiO$_2$ films (C and A) was determined to be 0.395 ± 0 and 0.700 ± 0.001 mg and 0.610 ± 0 and 0.950 ± 0 mg under UV-C and dark conditions. For the nanocomposite films TiO$_2$/Ag (H and G) their mass was measured to be 0.285 ± 0 and 0.545 ± 0 mg and 0.250 ± 0 and 0.360 ± 0 mg under dark and UV-C conditions, respectively.

The nanocomposite and pristine films (Ag/TiO$_2$, TiO$_2$/Ag, Ti, and Ag) showed significantly lower adhesion with *Scenedesmus* sp. compared to *Chlorella* sp. under both UV-C and dark conditions at all exposure concentrations ($P < 0.001$). A concentration-dependent decrease in the mass of the pristine TiO$_2$ films was observed upon exposure to *Chlorella* sp. and *Scenedesmus* sp. under UV-C and dark conditions, which was statistically significant ($P < 0.001$). Similarly, the pristine Ag films showed a significant difference between the exposure concentrations under both UV-C and dark conditions for both species ($P < 0.001$).

As the concentration of TiO$_2$ NPs increased (Ag NPs constant), the mass of *Chlorella* sp. and *Scenedesmus* sp. adhering on the films also decreased significantly ($P < 0.001$) under both UV-C and dark conditions for the nanocomposite Ag/TiO$_2$ films (A, B and C). Similarly, as the concentration of Ag NPs increased (TiO$_2$ NPs constant), the nanocomposite TiO$_2$/Ag films (G and H) also showed a significant reduction in adhesion under both UV-C and dark conditions ($P < 0.001$). There was a significant difference in adhesion of algae between the nanocomposite films of Ag/TiO$_2$ (A, B, and C) and TiO$_2$/Ag (G, H) under both UV-C and dark conditions ($P < 0.001$).

3.3 EPS formation

EPS production was evaluated after the interaction period (72 h) under dark and UV-C conditions (Fig. 4). The amount of EPS produced by *Scenedesmus* sp. upon interaction with the nanocomposite films of Ag/TiO$_2$ (A, B and C) was observed to be 0.075 ± 0.002, 0.08 ± 0.001 and 0.093 ± 0.004 mg mL^{-1} in the dark and 0.091 ± 0.003, 0.12 ± 0.001 and 0.13 ± 0.002 mg mL^{-1} under UV-C irradiation, respectively. The EPS produced by the nanocomposite TiO$_2$/Ag films (H and G) was observed to be 0.109 ± 0.003 and 0.076 ± 0.001 mg mL^{-1} and 0.088 ± 0.001 and 0.056 ± 0.001 mg mL^{-1} under UV-C and dark conditions, respectively. The pristine TiO$_2$ films (D, E and F) produced EPS under the irradiation of UV-C (0.089 ± 0.002, 0.1 ± 0.002 and 0.107 ± 0.002 mg mL^{-1}) and in the dark (0.069 ± 0.002, 0.078 ± 0.002 and 0.082 ± 0.003 mg mL^{-1}), respectively. For the pristine Ag (I, J and K) films, the amount of EPS produced was found to be 0.06 ± 0.003, 0.065 ± 0.003 and 0.078 ± 0.002 mg mL^{-1} and 0.067 ± 0.004, 0.076 ± 0.002 and 0.083 ± 0.002 mg mL^{-1} under UV-C and dark conditions, respectively.
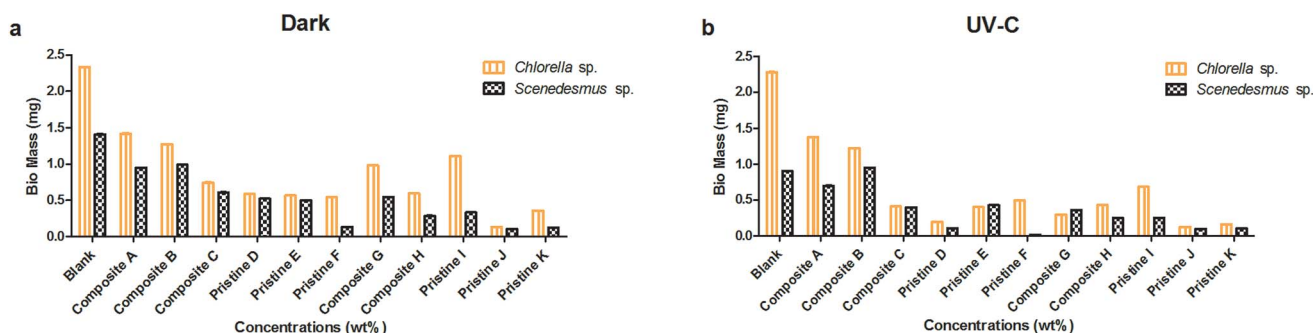

Fig. 3 Mass of the nanocomposite and pristine films interacted with *Chlorella* and *Scenedesmus* sp. under (a) dark and (b) UV-C conditions. The data are presented as mean $\pm$ SE, $n = 3$. Asterisks represent the level of significance ($P < 0.01$) between *Chlorella* and *Scenedesmus* sp.
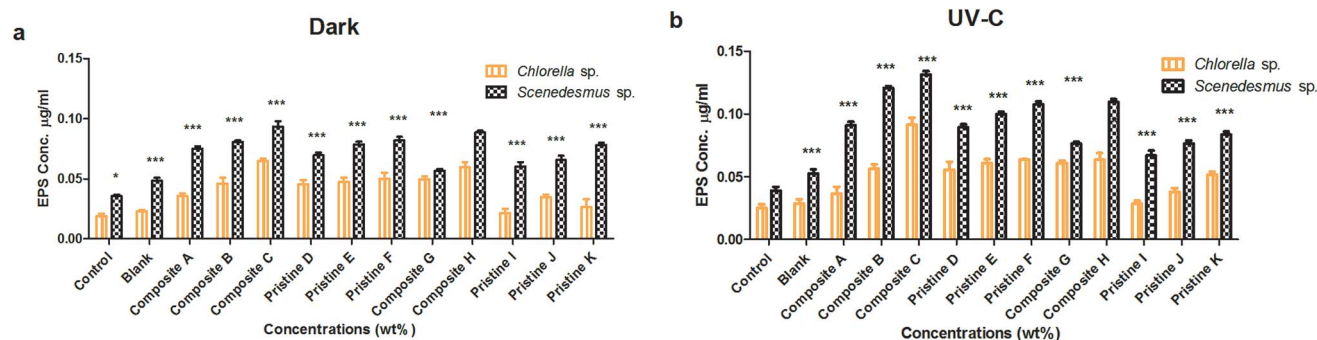
Fig. 4 EPS quantification in *Chlorella* and *Scenedesmus* sp. upon interaction with the nanocomposite and pristine films under (a) dark and (b) UV-C conditions. The data are presented as mean ± SE, $n = 3$. Asterisks represent the level of significance ($P < 0.01$) between *Chlorella* and *Scenedesmus* sp.

For *Chlorella* sp., the quantified EPS on the nanocomposite Ag/TiO$_2$ films (A, B and C) was found to be 0.035 ± 0.002, 0.046 ± 0.005 and 0.065 ± 0.002 mg mL^{-1} and 0.036 ± 0.005, 0.056 ± 0.003 and 0.091 ± 0.005 mg mL^{-1} under dark and UV-C conditions, respectively. For the nanocomposite TiO$_2$/Ag films (H and G), the amount of EPS produced was determined to be 0.06 ± 0.004 and 0.049 ± 0.002 mg mL^{-1} and 0.063 ± 0.005 and 0.061 ± 0.002 mg mL^{-1} under dark and UV-C conditions, respectively. The pristine TiO$_2$ film (D, E and F) produced EPS of about 0.045 ± 0.003, 0.047 ± 0.003 and 0.05 ± 0.005 mg mL^{-1} and 0.055 ± 0.006, 0.061 ± 0.003 and 0.063 ± 0 mg mL^{-1} under dark and UV-C conditions, respectively. For the pristine Ag films (I, J and K), the EPS quantified in the dark was 0.021 ± 0.003, 0.034 ± 0.002 and 0.026 ± 0.006 mg mL^{-1} and that under UV-C was 0.028 ± 0.002, 0.038 ± 0.003 and 0.051 ± 0.002 mg mL^{-1} conditions, respectively.

The nanocomposite (Ag/TiO$_2$ and TiO$_2$/Ag) and pristine films (TiO$_2$ and Ag) showed significantly higher EPS production for *Scenedesmus* sp. compared to *Chlorella* sp. under both UV-C and dark conditions at all exposure concentrations ($P < 0.001$). A concentration-dependent increase in EPS production for *Chlorella* sp. was observed upon exposure to the pristine TiO$_2$ films, which was found to be statistically significant under UV-C and dark conditions ($P < 0.001$). In contrast, the pristine Ag films did not show any significant difference between the exposure concentrations under both UV-C and dark conditions for *Chlorella* sp. ($P > 0.05$), whereas the pristine Ag film K showed a significant increase compared to that of the other pristine Ag films (J and I) under dark conditions for *Chlorella* sp. Exposure of *Scenedesmus* sp. to the pristine TiO$_2$ films resulted in a concentration-dependent increase in EPS production under both UV-C and dark conditions ($P < 0.001$); however, the pristine TiO$_2$ film F did not show a significant difference compared to pristine E under both conditions. The Ag pristine films showed a significant difference between the concentrations ($P < 0.001$) (except the pristine Ag film J compared to I under dark conditions and the pristine Ag film K compared to pristine Ag film J under UV-C condition showed an insignificant difference ($P > 0.05$) increase).

As the concentration of the TiO$_2$ NPs increased (Ag NPs constant), the production of EPS on *Scenedesmus* sp. also

increased significantly ($P < 0.001$) under both UV-C and dark conditions (Ag/TiO$_2$ nanocomposite films); except the nanocomposite film B exhibited an insignificant difference compared to A under dark conditions for *Scenedesmus* sp. ($P > 0.05$). Similarly, as the concentration of the Ag NPs increased (TiO$_2$ NPs constant) the nanocomposite TiO$_2$/Ag films (H and G) showed an increase in EPS production under both UV-C and dark conditions ($P < 0.001$). For *Chlorella* sp., as the concentration of the TiO$_2$ NPs increased (Ag NPs constant), the production of EPS also increased significantly ($P < 0.001$) under both UV-C and dark conditions, whereas the nanocomposite film A showed an insignificant difference compared to nanocomposite B under dark conditions ($P > 0.05$). As the concentration of the Ag NPs increased (keeping the concentration of the TiO$_2$ NPs constant), the nanocomposite TiO$_2$/Ag films (G and H) showed an increase in EPS production under both UV-C and dark conditions ($P < 0.001$). There was a significant difference between the nanocomposite films of Ag/TiO$_2$ (A, B, and C) and TiO$_2$/Ag (G and H) under both UV-C and dark conditions ($P < 0.001$), except for the nanocomposite Ag/TiO$_2$ film C, which showed an insignificant difference compared to the nanocomposite TiO$_2$/Ag film G under both conditions.

3.4 Cell surface damage

Lipid peroxide release was analyzed (Fig. 5) under dark and UV-C conditions for *Chlorella* sp. and *Scenedesmus* sp. after the 72 h interaction period. The pristine TiO$_2$ films of F and D showed LPO release of about 0.03 ± 0.001% and 0.023 ± 0.003% and 0.063 ± 0.007% and 0.034 ± 0.003% under the dark and UV-C conditions, respectively. The pristine Ag films of K and I showed LPO release, which was measured to be 0.022 ± 0.001% and 0.016 ± 0.001% and 0.045 ± 0.004% and 0.037 ± 0.005% under dark and UV-C conditions, respectively. LPO release was noted to be 0.076 ± 0.009% and 0.032 ± 0.003% and 0.0635 ± 0% and 0.027 ± 0.006% for the nanocomposite Ag/TiO$_2$ films of C and A under UV-C and dark conditions, respectively. The nanocomposite TiO$_2$/Ag films H and G showed the LPO release of 0.033 ± 0.008% and 0.027 ± 0.006% and 0.058 ± 0.009% and 0.044 ± 0.002% under dark and UV-C conditions, respectively.
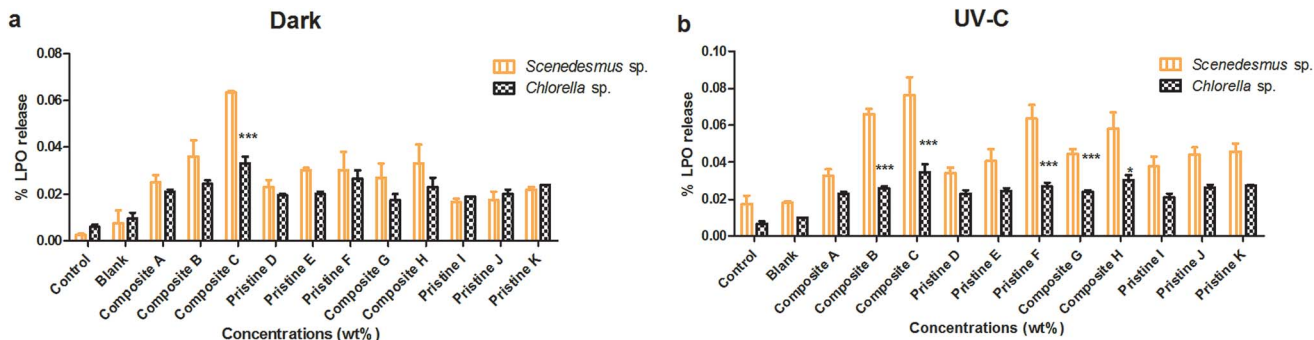
Fig. 5 Lipid peroxidation production in *Scenedesmus* and *Chlorella* sp. upon interaction with the nanocomposite and pristine films under (a) dark and (b) UV-C conditions. The data are presented as mean ± SE, $n = 3$. Asterisks represent the level of significance ($P < 0.01$) between *Scenedesmus* and *Chlorella* sp.

LPO release from *Chlorella* sp. was also studied upon exposure to the pristine TiO_2 film of F and D. The LPO release was observed to be 0.027 ± 0.002% and 0.023 ± 0.002% and 0.026 ± 0.003% and 0.019 ± 0% under UV-C and dark conditions, respectively. The pristine Ag films of K and I showed LPO release of about 0.027 ± 0% and 0.019 ± 0% and 0.024 ± 0 and 0.021 ± 0.002% under dark and UV-C conditions, respectively. The nanocomposite Ag/TiO_2 films of C and A showed the LPO release of about 0.034 ± 0.004% and 0.021 ± 0.001% and 0.033 ± 0.003% and 0.021 ± 0.001% under UV-C and dark conditions, respectively. The nanocomposite TiO_2/Ag films of H and G showed the LPO release of about 0.023 ± 0.004% and 0.017 ± 0.002% and 0.034 ± 0.004% and 0.024 ± 0.001% under dark and UV-C conditions, respectively.

Both the nanocomposite (Ag/TiO_2 and TiO_2/Ag) and pristine films (TiO_2 and Ag) did not show any significant difference between *Scenedesmus* sp. compared to *Chlorella* sp. under both UV-C and dark conditions at all exposure concentrations ($P > 0.001$). The pristine Ag films did not showed any significant difference between the exposure concentrations under both UV-C and dark conditions for *Scenedesmus* sp. ($P > 0.05$) (except the pristine Ag film J exhibited a significance ($P < 0.001$) when compared with the pristine Ag film K). The exposure of *Chlorella* sp. to the pristine Ag and TiO_2 films did not result in any concentration-dependent increase in LPO production under both UV-C and dark conditions ($P > 0.05$).

As the concentration of the TiO_2 NPs increased (Ag NPs constant), the LPO release of *Chlorella* sp. and *Scenedesmus* sp. also increased insignificantly ($P > 0.05$) under both UV-C and dark conditions for the Ag/TiO_2 nanocomposite films A, B and C (except the nanocomposite Ag/TiO_2 film A showed a significance ($P < 0.001$) when compared with the Ag/TiO_2 nanocomposite film B under UV-C conditions and the nanocomposite Ag/TiO_2 film B showed a significance ($P < 0.001$) when compared with the Ag/TiO_2 nanocomposite film C in the dark). For *Chlorella* sp., as the concentration of the TiO_2 NPs increased (Ag NPs constant), the LPO release showed a significant increase ($P < 0.001$) under both conditions. Similarly, as the concentration of the Ag NPs increased (TiO_2 NPs constant), the nanocomposite TiO_2/Ag films (G and H) also showed an increase in LPO release under both UV-C and dark conditions ($P > 0.05$) (except the

nanocomposite TiO_2/Ag film G showed a significant difference compared to the nanocomposite Ag/TiO_2 film G under both conditions). There was no significant difference in LPO release between the nanocomposite films of Ag/TiO_2 (A, B, and C) and TiO_2/Ag (G and H) under both UV-C and dark conditions ($P > 0.05$), except the Ag/TiO_2 nanocomposite film A showed a significant difference compared to the TiO_2/Ag nanocomposite film H under dark conditions ($P < 0.001$).

3.5 Bio-uptake of Ti and Ag

Upon the interaction of the algal cells with two or more toxicants in the test systems, internalisation or uptake of leached nanoparticles can take place. The absorption of leached nanoparticles was evaluated under dark and UV-C conditions for *Chlorella* sp. and *Scenedesmus* sp. (Fig. 6). The highest TiO_2 uptake for *Chlorella* sp. with the nanocomposite Ag/TiO_2 (C) and TiO_2/Ag (H) films was observed to be 0.561 ± 0.058, 0.473 ± 0.023 µg mL^{-1} and 0.798 ± 0.011, 0.592 ± 0.061 µg mL^{-1} under dark and UV-C conditions, respectively. The TiO_2 internalization for *Scenedesmus* sp. with the nanocomposite films Ag/TiO_2 and TiO_2/Ag (C and H) in was determined to be 0.96 ± 0.02 and 0.703 ± 0.022 µg mL^{-1} and 0.81 ± 0.02 and 0.513 ± 0.008 µg mL^{-1} under UV-C and dark conditions, respectively.

The higher concentration nanocomposite films (Ag/TiO_2 and TiO_2/Ag) resulted in a significantly higher biouptake in *Scenedesmus* sp. compared to that of *Chlorella* sp. under both UV-C and dark conditions ($P < 0.001$). In contrast Ag uptake into *Chlorella* sp. upon exposure to the higher concentration nanocomposite films (Ag/TiO_2 and TiO_2/Ag) did not result in any significant difference between the UV-C and dark conditions ($P > 0.05$).

3.6 Dissolution of Ag$^+$ from nanocomposite film

The dissolution of Ag ions from the nanocomposite films was observed (Fig. 7) to be in the order of nanocomposite Ag/TiO_2 film C (0.394 ± 0.116 µg mL^{-1}) > nanocomposite film TiO_2/Ag H (0.203 ± 0.063 µg mL^{-1}) < pristine Ag film K (0.271 ± 0.036 µg mL^{-1}) under dark conditions. Under UV-C irradiation, Ag$^+$ leaching was observed to be in the order of pristine Ag film K (0.337 ± 0.083 µg mL^{-1}) > nanocomposite TiO_2/Ag film H (0.3 ±
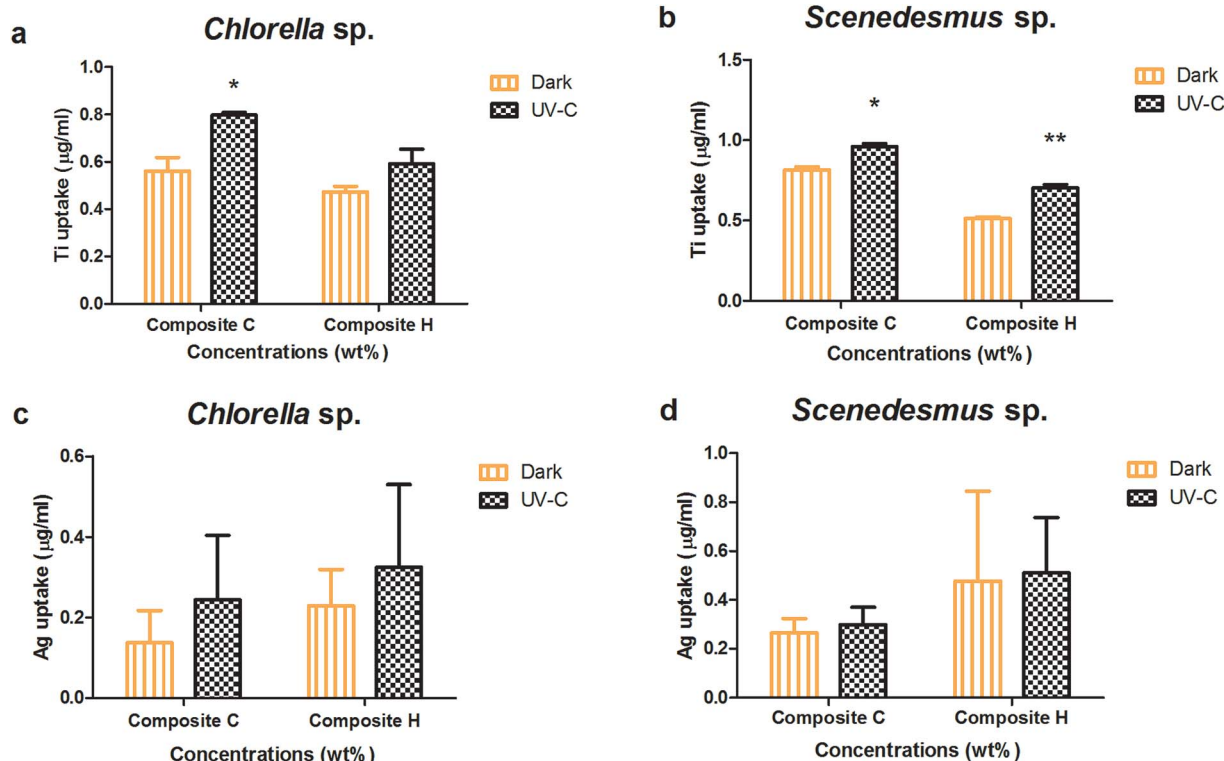
Fig. 6 Biouptake of TiO$_2$ and Ag nanoparticles on (a and c) *Chlorella* and (b and d) *Scenedesmus* sp. upon interaction with the nanocomposite films under dark and UV-C conditions. The data are presented as mean ± SE, $n = 3$. Asterisks represent the level of significance ($P < 0.01$) between dark and UV-C.
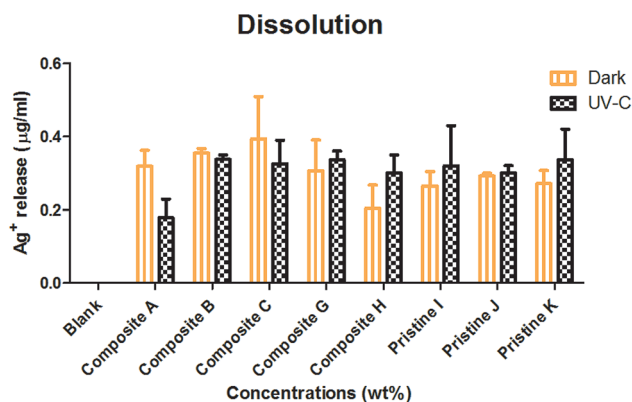

Fig. 7 Silver ion leaching measured under dark and UV-C conditions in BG-11 medium upon interaction with the nanocomposite and Ag pristine films. The data are presented as mean ± SE, $n = 3$.

0.05 μg mL^{-1}) < nanocomposite Ag/TiO$_2$ film C (0.325 ± 0.065 μg mL^{-1}). UV-C exposure resulted in more Ag$^+$ leaching compared to in the dark, except for the Ag/TiO$_2$ nanocomposite film C.

The nanocomposite (Ag/TiO$_2$ and TiO$_2$/Ag) and pristine films (Ag) showed an insignificant ($P > 0.05$) increase in dissolution under dark and UV-C conditions. The nanocomposite films (TiO$_2$/Ag) and (Ag/TiO$_2$) showed no significant difference between them ($P < 0.05$) under both conditions. There was no

significant difference between nanocomposite films ($P > 0.05$) under dark and UV-C conditions.

3.7 Changes in nanocomposite films as analyzed by XRD

The X-ray diffraction patterns of the pristine and nanocomposite films were observed before and after interaction with the algae. Fig. 8A and C show the XRD patterns of the Ag (0.5 mg L^{-1}) and TiO$_2$ (0.75 mg L^{-1}) pristine films, which exhibit peaks at $2\theta = 38°$ ($d_{001} = 111$ nm), $44°$ ($d_{001} = 200$) and $25.3°$ ($d_{001} = 101$) associated with the plane-oriented anatase structure of TiO$_2$ NPs. After interaction with the algal cells, there were no significant changes in the crystalline structure of the pristine Ag and TiO$_2$ films (Fig. 8B and D). The nanocomposite film (Fig. 8E) shows both crystalline peaks of Ag and TiO$_2$, and there were no changes upon exposure to the algal cells (Fig. 8F).

3.8 Changes in surface functional groups analyzed by FTIR

The functional groups of the nanocomposite films were analyzed using FTIR spectroscopy. The IR spectra of the nanocomposite films are depicted in Fig. 9. The Ag pristine film displays spectral (Fig. 9A) peaks at 2864 cm^{-1} (C–H stretch), 2360 cm^{-1} (C–N asymmetric band stretching), 1646 cm^{-1}, 1524 cm^{-1} (amide II band, C–O stretch of acetyl group), and 1072 cm^{-1} (skeletal vibration involving the bridge C–O stretch) of the glucosamine residue. The pristine Ag film interacted with *Chlorella* sp. displays a broader peak at 3290 cm^{-1} (O–H
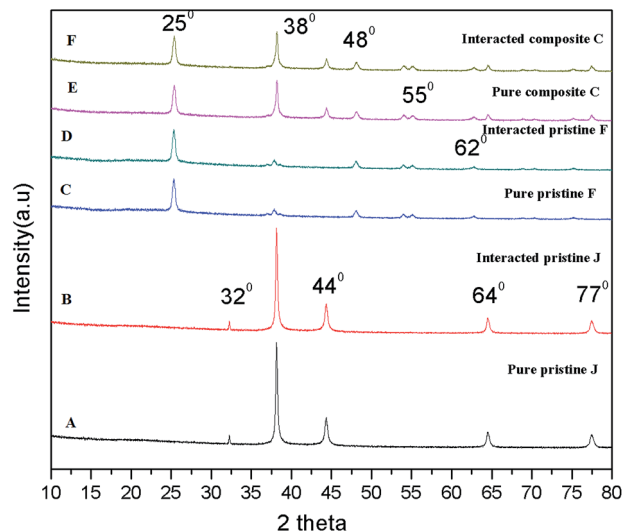
Fig. 8 X-ray diffraction patterns of the Ag pristine, TiO$_2$ pristine and TiO$_2$/Ag nanocomposite films upon interaction with *Scenedesmus* sp.

stretching of alcohols), which is associated with the cross-linkages between the amino groups in chitosan molecules. The peak at 1324 cm^{-1} indicates C–N stretching (amide II). The peak at 1368 cm^{-1} is assigned to acetamide groups, and the peaks at 1072 cm^{-1} and 1012 cm^{-1} are associated with the C–O stretching linkage observed upon interaction with *Scenedesmus* sp. The spectrum of the pristine TiO$_2$ film (Fig. 9B) shows a peak at 1525 cm^{-1} corresponding to the C–O stretch of the amide II band. The peak at 1400 cm^{-1} corresponds to the carboxylate groups associated with the antimicrobial activity of the biopolymer, which was shifted to 1361 cm^{-1} upon interaction with *Scenedesmus* sp. Fig. 9C displays peaks at 3518 cm^{-1} for the symmetrical N–H stretching vibration band, 1299 cm^{-1} for the C–S stretching frequency, and 1143 cm^{-1} (anti-symmetric stretching of the C–O–C bridge), which can be assigned to the saccharide structure.

4. Discussion

Polymers are the most popular materials used for the development of antifouling coatings due to their ease of application.[6,7] Chitosan nanocomposites have emerged with incredible applications such as enhanced antimicrobial and antifouling applications and in drug delivery systems.[9,25–27] In this study, the antifouling action of different nanoparticle-incorporated chitosan films was analyzed on two different algal species, namely, *Scenedesmus* sp. and *Chlorella* sp. All the nanocomposite and pristine (Ag/TiO$_2$, TiO$_2$/Ag, TiO$_2$, and Ag) films tested in this study exhibit enhanced algal toxicity towards both freshwater microalgae, *Scenedesmus* sp. and *Chlorella* sp. compared to their blank, *i.e.*, chitosan films. Ravikumar *et al.* (2000) reported the effect of chitosan on controlling the growth of algae.[28] In a recent study by Al-Namaani *et al.* (2017), a chitosan–ZnO nanocomposite coating on glass substrates amplified the anti-diatom activity of a chitosan coating towards the diatom

Navicula sp. Ren *et al.* (2014) elucidated that surface-modified Ag NPs reduce the attachment of algae on substrates. Among the pristine films, TiO$_2$ films portrayed higher toxicity than Ag films. It has been reported that the larger band gap energy of TiO$_2$ NPs diminishes the strength of fouling to a greater extent.[29,30] The plausible mechanism for Ag toxicity is typically due to the dissolution of Ag$^+$ ions from the films, in addition to their reactivity.[31]

Moreover, the type of irradiation greatly influences the toxicity of nanocomposite films. Both algal species showed higher toxicity under UV irradiation for all the films, especially the TiO$_2$ films. As expected, the nanocomposite films displayed enhanced toxicity especially under UV irradiation compared to the pristine films (both Ag and TiO$_2$ films) for both test organisms in this study. Presumably the ion release effects of Ag nanoparticles and photocatalytic activity of TiO$_2$ particles enhanced the algal toxicity of the chitosan films incorporated with Ag and TiO$_2$ NPs. The photocatalytic action of the TiO$_2$ films, both pristine as well as nanocomposite could be a prime reason behind their enhanced toxicity. Lee *et al.* (2015) reported an enhanced photocatalytic disinfection effect by silver NP-functionalized TiO$_2$ NPs on harmful algae, such as *Tetraselmis suecica* and *Amphidinium carterae*.[32]

In the recent years, new antifoulants have been developed based on three principal strategies: (i) counteracting the attachment of biofouling organisms on surfaces, (ii) mitigating the adherence of biofoulants and (iii) destroying biofoulants.[8] Algal fouling was evaluated in terms of slime formation to analyze the antifouling action of the films. Slime formation by *Chlorella* sp. was noted to be higher than *Scenedesmus* sp. even after interaction with the films. UV irradiation decreased the slime formation by both algal species to some extent, in response to the chitosan (nanocomposite as well as pristine) films. The hydrophilicity of the substrates (chitosan and photocatalytic metal oxides) was suspected to increase upon exposure to UV light, which thereby reduced the adhesion of cells. Furthermore, it is known that an increase in hydrophilicity augments the antifouling action of substrates.[1,33,34] The variation in the concentration of Ag or TiO$_2$ NPs in the nanocomposite films did not induce any significant changes in the slime formation of the algal species. In addition, the biomass% results reflect the difference in the attachment of algal cells on the films corresponding to the type of NPs incorporated. The biomass of *Scenedesmus* sp. was lower compared to that of *Chlorella* sp. The nanocomposite films were highly toxic to algal cells compared to the pristine films, especially under UV irradiation. The NP concentration in the films greatly influenced the decrement of biomass of algal cells on the films. Slime formation and biomass represent the adherence nature as well as attachment of microalgae on the film surfaces. These results confirm that the antifouling action of the nanoparticle-incorporated chitosan films in addition to their toxicity. Chapman *et al.* (2013) reported a decrease in the mass percent of MNP-doped films compared to their blanks, which signifies a reduction in the microbial attachment to the films and slime formation on the MNP-doped film.
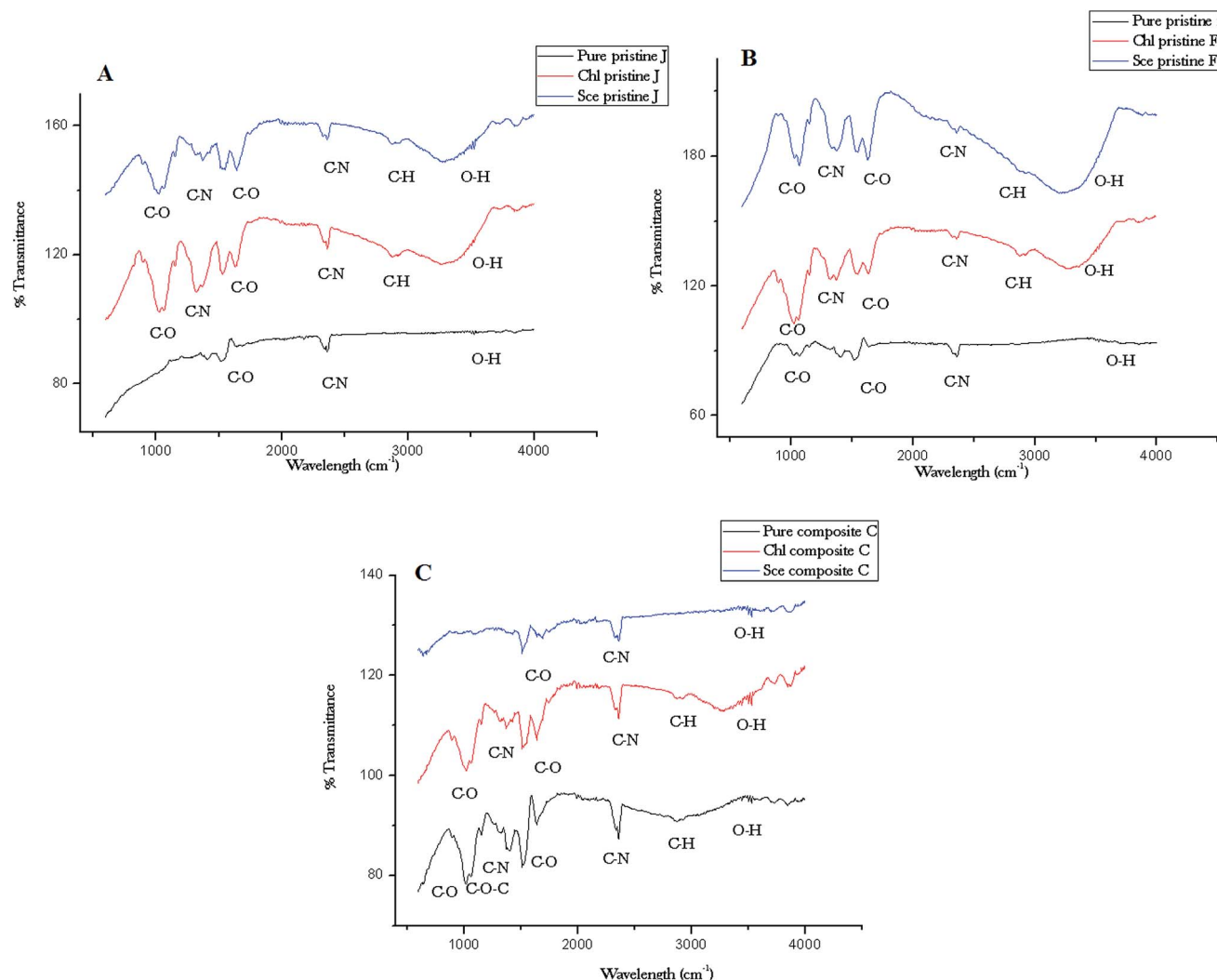
Fig. 9 ATR-FTIR spectra of the nanocomposite (C) and pristine (A and B) films before and after interaction with *Chlorella* and *Scenedesmus* sp. under UV-C irradiation.

The antifouling mechanism of the chitosan films was confirmed with extracellular polysaccharide (EPS) and cell membrane damage (LPO) assays. The EPS release by *Scenedesmus* sp. and *Chlorella* sp. well corroborate the toxicity results obtained under UV and dark conditions. The EPS release was higher for the nanocomposite films than the pristine films, especially under UV irradiation. The algal cells produced more EPS to counteract the stress induced by the films. A similar increase in EPS was noted by Mohammad (2008) on *Scenedesmus quadricauda* and *Chlorella vulgaris* upon interaction with microcystins, who also reported that the polysaccharides produced by algal cells reduce the oxidative stress induced by microcystins.[35] LPO production by algal cells was found to be unique for all the films tested (Ag, TiO$_2$, Ag/TiO$_2$ and TiO$_2$/Ag) and dependent on the type of film, both nanocomposite and pristine films, and based on the type of irradiation. The only difference noted between *Scenedesmus* sp. and *Chlorella* sp. was that the former showed a higher LPO production than the latter in relation to its higher toxicity. The lipid peroxidation results

indicate an increase in the membrane permeability of the cells as a consequence of cell wall damage due to the oxidative stress induced by the NPs.[36]

The NP internalisation data reveal that the uptake of TiO$_2$ NPs was highly preferred by both algal species rather than Ag NPs under both UV and dark conditions. *Scenedesmus* sp. showed a higher uptake under UV irradiation in relation to their toxicity. Although the silver NPs were soluble, the Ag NP uptake was noted to be constant regardless of the exposure conditions. The dissolution studies further revealed the reason behind the lower uptake of Ag NPs, which show that the dissolution of Ag ions from the films was independent of exposure conditions as well as concentration.

Among the two species tested in this study, *Scenedesmus* sp. showed a higher sensitivity to all the films tested than *Chlorella* sp. under both exposure conditions (UV and dark). The results of the slime formation, biomass%, LPO, and uptake of NPs were well corroborated with the toxicity data. EPS release was noted to be higher for *Scenedesmus* sp. than *Chlorella* sp., in relation to

the higher toxicity of the former algal species. This indicates that the species variation substantially influences the anti-fouling action of chitosan films, both pristine as well as nano-composite. These toxicity differences due to variation in characteristics of the algae such as morphology, physiology, cytology, and genetics[37,38] despite exposure to the same toxicant can be informative.

5. Conclusion

Among the two algal species examined, *Scenedesmus* sp. was found to be more sensitive to all the films tested than *Chlorella* sp. under both UV-C exposure and dark conditions. Similarly, the slime formation, biomass (%), LPO, and uptake of NPs are in accordance with their toxicity data. EPS release was noted to be higher for *Scenedesmus* sp. than *Chlorella* sp. in relation to the higher toxicity of the former algal species. This indicates that the species variation substantially influences the antifouling action of chitosan films, both pristine as well as nanocomposite.

Acknowledgements

References

1 R. Dineshram, R. Subasri, K. Somaraju, K. Jayaraj, L. Vedaprakash, K. Ratnam, S. Joshi and R. Venkatesan, *Colloids Surf., B*, 2009, **74**, 75–83.

2 E. Martinelli, M. Suffredini, G. Galli, A. Glisenti, M. E. Pettitt, M. E. Callow, J. A. Callow, D. Williams and G. Lyall, *Biofouling*, 2011, **27**, 529–541.

3 J. Chapman, L. Le Nor, R. Brown, E. Kitteringham, S. Russell, T. Sullivan and F. Regan, *J. Mater. Chem. B*, 2013, **1**, 6194–6200.

4 J. Ren, P. Han, H. Wei and L. Jia, *ACS Appl. Mater. Interfaces*, 2014, **6**, 3829–3838.

5 K. Thomas and S. Brooks, *Biofouling*, 2010, **26**, 73–88.

6 H. Murata, R. R. Koepsel, K. Matyjaszewski and A. J. Russell, *Biomaterials*, 2007, **28**, 4870–4879.

7 M. Malini, M. Thirumavalavan, W.-Y. Yang, J.-F. Lee and G. Annadurai, *Int. J. Biol. Macromol.*, 2015, **80**, 121–129.

8 W. J. Yang, K.-G. Neoh, E.-T. Kang, S. L.-M. Teo and D. Rittschof, *Prog. Polym. Sci.*, 2014, **39**, 1017–1042.

9 L. Al-Naamani, S. Dobretsov, J. Dutta and J. G. Burgess, *Chemosphere*, 2017, **168**, 408–417.

10 J. M. Lagaron, M. J. Ocio and A. Lopez-Rubio, *Antimicrobial polymers*, John Wiley & Sons, 2011.

11 K. Muraleedaran and V. A. Mujeeb, *Int. J. Biol. Macromol.*, 2015, **77**, 266–272.

12 S. Saravanan, S. Nethala, S. Pattnaik, A. Tripathi, A. Moorthi and N. Selvamurugan, *Int. J. Biol. Macromol.*, 2011, **49**, 188–193.

13 M. Yadollahi, S. Farhoudian and H. Namazi, *Int. J. Biol. Macromol.*, 2015, **79**, 37–43.

14 A. G. Agrios and P. Pichat, *J. Appl. Electrochem.*, 2005, **35**, 655–663.

15 S. Eyssautier-Chuine, M. Gommeaux, C. Moreau, C. Thomachot-Schneider, G. Fronteau, J. Pleck and B. Kartheuser, *Q. J. Eng. Geol. Hydrogeol.*, 2014, **47**, 177–187.

16 J. G. McEvoy and Z. Zhang, *J. Photochem. Photobiol., C*, 2014, **19**, 62–75.

17 M. Bhuvaneshwari, V. Iswarya, S. Archanaa, G. Madhu, G. S. Kumar, R. Nagarajan, N. Chandrasekaran and A. Mukherjee, *Aquat. Toxicol.*, 2015, **162**, 29–38.

18 V. Iswarya, M. Bhuvaneshwari, S. A. Alex, S. Iyer, G. Chaudhuri, P. T. Chandrasekaran, G. M. Bhalerao, S. Chakravarty, A. M. Raichur and N. Chandrasekaran, *Aquat. Toxicol.*, 2015, **161**, 154–169.

19 V. Iswarya, J. Johnson, A. Parashar, M. Pulimi, N. Chandrasekaran and A. Mukherjee, *Environ. Sci. Pollut. Res.*, 2016, 1–12.

20 S. Dalai, S. Pakrashi, M. J. Nirmala, A. Chaudhri, N. Chandrasekaran, A. Mandal and A. Mukherjee, *Aquat. Toxicol.*, 2013, **138**, 1–11.

21 A. Piotrowska-Niczyporuk, A. Bajguz, E. Zambrzycka and B. Godlewska-Żyłkiewicz, *Plant Physiol. Biochem.*, 2012, **52**, 52–65.

22 M. DuBois, K. A. Gilles, J. K. Hamilton, P. Rebers and F. Smith, *Anal. Chem.*, 1956, **28**, 350–356.

23 J. Chapman, C. Hellio, T. Sullivan, R. Brown, S. Russell, E. Kiterringham, L. Le Nor and F. Regan, *Int. Biodeterior. Biodegrad.*, 2014, **86**, 6–13.

24 S. Natarajan, M. Bhuvaneshwari, D. S. Lakshmi, P. Mrudula, N. Chandrasekaran and A. Mukherjee, *Environ. Sci. Pollut. Res.*, 2016, **23**, 19529–19540.

25 G. Mendoza, A. Regiel-Futyra, V. Andreu, V. c. Sebastián, A. Kyzioł, G. y. Stochel and M. Arruebo, *ACS Appl. Mater. Interfaces*, 2017, DOI: 10.1021/acsami.6b15123.

26 H. Zhang, T. Yan, S. Xu, S. Feng, D. Huang, M. Fujita and X.-D. Gao, *Mater. Sci. Eng., C*, 2017, **73**, 144–151.

27 A. M. Youssef, H. Abou-Yousef, S. M. El-Sayed and S. Kamel, *Int. J. Biol. Macromol.*, 2015, **76**, 25–32.

28 M. N. R. Kumar, *React. Funct. Polym.*, 2000, **46**, 1–27.

29 U. Diebold, *Surf. Sci. Rep.*, 2003, **48**, 53–229.

30 Z. Zhang, J. MacMullen, H. N. Dhakal, J. Radulovic, C. Herodotou, M. Totomis and N. Bennett, *Build. Sci.*, 2013, **59**, 47–55.

31 D. He, J. J. Dorantes-Aranda and T. D. Waite, *Environ. Sci. Technol.*, 2012, **46**, 8731–8738.

32 S.-W. Lee, S. Obregón and V. Rodríguez-González, *RSC Adv.*, 2015, **5**, 44470–44475.

33 B. Li and B. E. Logan, *Colloids Surf., B*, 2005, **41**, 153–161.

34 T. Abiraman, E. Ramanathan, G. Kavitha, R. Rengasamy and S. Balasubramanian, *Ultrason. Sonochem.*, 2017, **34**, 781–791.

35 Z. A. Mohamed, *Ecotoxicology*, 2008, **17**, 504.

36 N. von Moos and V. I. Slaveykova, *Nanotoxicology*, 2014, **8**, 605–630.

37 F. Kasai and S. Hatakeyama, *Chemosphere*, 1993, **27**, 899–904.

38 R. A. Kent and D. Currie, *Environ. Toxicol. Chem.*, 1995, **14**, 983–991.